

ARTICLE

Monitoring Heart Rate Variability Based on Self-powered ECG Sensor Tag

Nhat Minh Tran¹ Ngoc-Giao Pham² Thang Viet Tran^{3*}

1. Department of Telecommunication, Sai Gon University, Vietnam

2. Department of Computing Fundamentals, FPT University, Hanoi, Vietnam

3. Department of Science and Technology, Nguyen Tat Thanh University, Ho Chi Minh City, Vietnam

ARTICLE INFO

Article history

Received: 1 November 2022

Revised: 9 November 2022

Accepted: 14 November 2022

Published Online: 25 November 2022

Keywords:

Batteryless ECG sensor

Heart rate monitoring

UHF RFID

ABSTRACT

This paper proposes a batteryless sensing and computational device to collect and process electrocardiography (ECG) signals for monitoring heart rate variability (HRV). The proposed system comprises of a passive UHF radio frequency identification (RFID) tag, an extreme low power microcontroller, a low-power ECG circuit, and a radio frequency (RF) energy harvester. The microcontroller and ECG circuits consume less power of only $\sim 30 \mu\text{A}$ and $\sim 3 \text{ mA}$, respectively. Therefore, the proposed RF harvester operating at frequency band of $902 \text{ MHz} \sim 928 \text{ MHz}$ can sufficiently collect available energy from the RFID reader to supply power to the system within a maximum distance of $\sim 2 \text{ m}$. To extract R-peak of the ECG signal, a robust algorithm that consumes less time processing is also developed. The information of R-peaks is stored into an Electronic Product Code (EPC) Class 1st Generation 1st compliant ID of the tag and read by the reader. This reader is functioned to collect the R-peak data with sampling rate of 100ms ; therefore, the user application can monitor fully range of HRV. The performance of the proposed system shows that this study can provide a good solution in paving the way to new classes of healthcare applications.

1. Introduction

Wearable wireless body devices are widely deployed in health monitoring system nowadays. However, most of the distributed body sensor nodes consume more power due to wireless data transmission power^[1-3]. To overcome the serious drawback in specific applications, in this work,

the UHF RFID technology that does not require power to communicate with base station is considered instead of conventional wireless methods such as the ZigBee, BlueTooth, and WiFi standards. In addition, a RF energy harvester was designed to collect RF energy that is come from RFID reader for supplying power to the ECG sensor module. Therefore, the proposed system can power inde-

*Corresponding Author:

Thang Viet Tran,

Department of Science and Technology, Nguyen Tat Thanh University, Ho Chi Minh City, Vietnam;

Email: tvthang@ntt.edu.vn

DOI: <https://doi.org/10.30564/jeis.v4i2.5225>

Copyright © 2022 by the author(s). Published by Bilingual Publishing Co. This is an open access article under the Creative Commons Attribution-NonCommercial 4.0 International (CC BY-NC 4.0) License. (<https://creativecommons.org/licenses/by-nc/4.0/>).

pendently in normal operation duration.

HRV is one of critical parameters to diagnose a number of medical conditions, including diabetes, sleep apnea, cardiovascular diseases, and mental stress^[4]. HRV measurements are basically extracted from original ECG signals that are collected by wearable devices. These wearable devices traditionally transmitted data to the host over Bluetooth, ZigBee, or WiFi links^[5]. However, some wearable sensors for measuring the biomedical signals showed that the power consumption of wireless standards consumes significant average power of 14.8 mW and 30.7 mW in Bluetooth low energy (BLE) and ZigBee, respectively^[6]. In actual cases, assisted battery-based wearable devices need to replace battery after dozens of operating hours due to high wireless transmission power. Therefore, a compact, long life, real-time HVR assessment device has to be designed to enable and expand HVR diagnostic applications in future.

Recently RFID has become the critical component in the design of various applications in industries and social life. Emerging RFID applications extend from tracking areas, cold chain management, and patient identification^[7], to battery-less sensing applications using RF energy harvester. A low-cost and battery-less smart sensor tag operating at high frequency (HF) can measure temperature and relative humidity within distance of 30 cm for monitoring the freshness of packaged vegetable. To monitor temperature and humidity in far distance of 27 m in outdoor environment, a long-range UHF RFID tag with assisted solar panel was developed. Moreover, RFID sensor tag can be used to collect physiological signals from human body. A wearable UHF RFID-based smart tag that does not require battery can monitor electroencephalogram (EEG) signal at the distances up to 0.8 m. The autonomous sensor tags that operate at UHF band can measure ECG signals for monitoring HR and HRV^[8]. The structure of our paper is organized as follows: Section 2 presents the related works; Section 3 introduces a system design; Section 3 gives an explanation of the proposed algorithm; Section 4 describes experimental results; and conclusions is shown in Section 5.

2. Related Works

2.1 UHF RFID System

Basically, the RFID systems consist of small low-cost, wireless battery-free devices, called tags, which use the radio signal from a specialized RFID reader for power and communication. When queried, each tag responds to a unique identification number by reflecting energy back

to the reader through backscatter modulation. Tags are often application-specific fixed-function devices that have a range of 10 cm ~ 50 cm for high frequency (HF) devices and 3 m ~ 10 m for UHF tags^[9,10]. The development of RFID technology has produced a robust physical layer capable of wirelessly powering and querying a tag. This core technology enables a new class of wireless battery-free devices with communication. This study just focuses on design of the UHF RFID-based sensor tag that operates at frequency of ~915 MHz.

2.1.1 Types of RFID Tags

Typically there are three types of RFID tags, namely, passive, semi-passive, and active tags^[11]. The operation of each is shown in Figure 1.

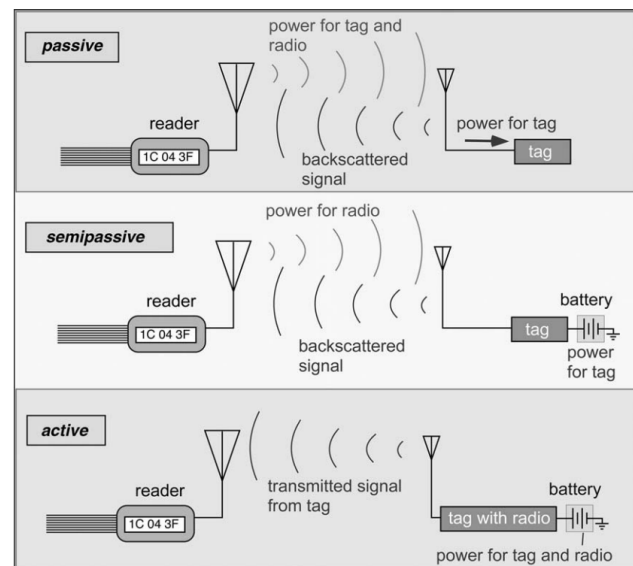


Figure 1. Configuration of three types of tags

Passive tag: This type of tags contains no power supply on board; therefore, they are very cheap and small. Passive tags absorb their energy when they enter an electromagnetic field (also called Near Field) created by RFID reader's antenna. The Near Field can be proximately calculated by the following equation: $r = \lambda / (2 * \pi)$, where λ is the wavelength. Due to the reason of no power supplied on board, the read range of passive tags is very short of several mm. Once a RFID reader has interrogated passive tags, and passive tags have absorbed enough energy, they use backscatter which is an RF technique to send their data back to RFID reader.

Semi-passive tag: The main difference is to require battery compared with passive tag. Batteries in semi-passive tags are only used to power the internal circuitry. The semi-passive tags still need to be presented inside the Near Filed in order to absorb power for data transmission

between RFID readers and themselves. The advantage of semi-passive tags is longer read ranges than passive tags because the energy they absorb from Near Field is fully used to transmit data only. Batteries in semi-active tags are used exactly the same as those in active tags; however, the energy will only be released to power the tags when the tags are being interrogated by RFID readers.

Active tag: Unlike passive tags, this type of tags comes with power supplied on board such as battery. Since they have their own power supply, they do not need to be powered by the Near Field of RFID readers' antennas. Therefore, passive tags have longer read range than passive tag. The drawbacks are that they are more expensive and bigger in size. Active tags send out signals which are encoded with their identifiers at regularly scheduled rate usually between 1 to 15 seconds.

2.1.2 UHF RFID Air Communication Protocol

There are two main air communication protocols that are involved in developing standards for UHF RFID technology, namely, EPCglobal (electronic product code) GEN2 (second-generation) and ISO (international standard organization) 1800-Part 6. In this study, the EPCglobal GEN2 is only considered due to the proposed application.

EPCglobal is a joint venture between Uniform Code Council (UCC) and EAN International. The organization carries the mission of the former Auto-ID (auto identification) Center at MIT (Massachusetts Institute of Technology). It is primarily goal is to make the final EPC standard an official global standard. The EPC class types are summarized in Table 1 and an example of Electronic Product Code (EPC) structure is presented in Table 2 [12].

Table 1. EPC class types

EPC class type	Feature	Tag type
Class 0	Read only	Passive (64 bits only)
Class 1	Write one/ Read many	Passive (96 bits minimum)
Class 2	Read/Write	Passive (96 bits minimum)
Class 3	Read/Write with battery power to enhance range	Semi-active
Class 4	Read/Write active transmitter	Active

2.1.3 Read Range Calculation

To calculate the reading range from the reader to the tag in frequency range of UHF band we can use the Friis equation. With the Friis equation, we can immediately draw the reversed link diagram for a directional antenna: the

received power is simply increased by antenna again [11]. The results are shown in Figure 2.

Table 2. EPC code structure

Code	Representation
01	Version of EPC (8 bits header)
115A1D7	Manufacture Identifier; 28 bit (> 16 million possible manufactures)
28A1E6	Product Identifier; 24 bit (> 16 million possible products per manufacture)
421CBA30A	Item Serial Number; 36 bit (> 68 billion possible unique items per product)

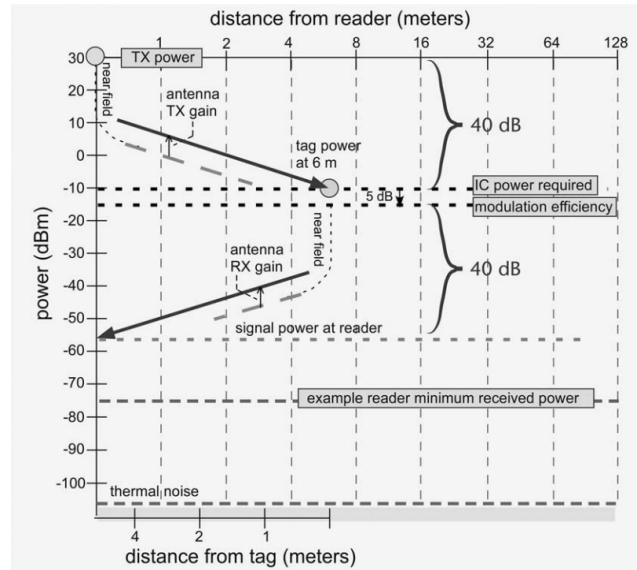


Figure 2. Forward and reverse link budgets for directional antenna

The received power is the same as in the isotropic case, even though the tag is twice as far away because the power at the tag is the same in both cases, and the received power is decreased by 6 dB due to the larger distance but increased by 6 dB due to the receiver antenna again. We can also construct a mathematical statement of the same relationships using the Friis equation by defining the gain of the tag antenna G_{tag} and a backscatter transmission loss $T_b (= 1/3 \text{ or } -5 \text{ dB})$. Then we have:

$$P_{TX,tag} = P_{TX,reader} G_{reader} G_{tag} \left(\frac{\lambda}{4\pi r} \right)^2 T_b \quad (1)$$

$$P_{RX,reader} = P_{TX,tag} G_{tag} G_{reader} \left(\frac{\lambda}{4\pi r} \right)^2 \quad (2)$$

$$P_{RX,reader} = P_{TX,reader} T_b G_{reader}^2 G_{tag}^2 \left(\frac{\lambda}{4\pi r} \right)^4 \quad (3)$$

In the most general case, the power received at the reader does as the inverse fourth power of (> the distance). It is also

proportional to the square of the antenna gains, so when reverse link power is important such as passive tag, the antenna gain plays a very large role in achievable read range. Real tag antennas have some gain, but it is typically modest (around 2 dB, since they are usually dipole-like), and since the application do not always control the exact orientation of the tag antenna and may not be able to guarantee that the main beam of the tag antenna is pointed at the reader, it is prudent to count on minimal gain from the tag antenna.

Using the Friis equation, we can also provide a couple of convenient range equations that can be useful for quick estimates. First, defining the minimum power, the tag requires as $P_{\min, \text{tag}}$, therefore the forward-link-limited range can be obtained:

$$R_{\text{forward}} = \left(\frac{\lambda}{4\pi} \right) \sqrt{\frac{P_{\text{TX}} G_{\text{reader}} G_{\text{tag}}}{P_{\min, \text{tag}}}} \quad (4)$$

and defining the minimum signal power for demodulation at the reader as $P_{\min, \text{rdr}}$, the reverse-link-limited range can be obtained:

$$R_{\text{reverse}} = \left(\frac{\lambda}{4} \right) \sqrt{\frac{P_{\text{TX}, \text{reader}} T_b G_{\text{reader}}^2 G_{\text{tag}}^2}{P_{\min, \text{rdr}}}} \quad (5)$$

2.2 Real-time ECG R-peak Detection Algorithm

Traditionally ECG waveforms are usually recorded in a clinical setting by medical professionals using twelve leads attached to the patient [13]. This work has developed a three-lead ECG device for use by person at home. The ECG signals recorded by human body with a three-lead suffer greatly from baseline wandering and high frequency noises, as compared to ECG signals recorded with twelve-leads in a clinical setting. Therefore, an accurate R-peak detection algorithm is an important step in ECG analysis. Various methods have been proposed in the past to detect R-peak under challenge conditions by using wavelet transform or Hilbert transform [14-16]. However, abovementioned methods consume more processing time and that suite to be applied in PC application or high-speed smart phones. In this study, we propose a new real-time R-peak detection algorithm for three-lead mobile ECG recordings. The proposed algorithm is simple to implement, computationally efficient, and does not require any signal pre-processing. This conceptual simplicity is a quality that distinguishes our approach from existing solutions. And therefore, the proposed algorithm consumes less processing time and can easily be applied into firmware for low-speed MCU based applications.

2.2.1 Characteristics of ECG Waveforms under Challenge Conditions

Recording ECG waveforms under motion artifacts and

respiration conditions causes the signals containing data losses, low and high frequency noises. Figure 3 shows an example of the ECG waveforms with data loss. Therefore the R-R interval in case of data loss is difficult to release by conventional R-peak detection method. Basically, the ECG comprises four different waves, namely, Q-wave, R-wave, S-wave, and T-wave; among them, R-wave and T-wave have higher amplitude compared to others. Most of cases, R-wave amplitude is bigger than T-wave. However, in specific case, as shown in Figure 4, the T-wave amplitude can compare with R-wave due to motion artifacts or respiration conditions. In this case, the R-peak detection method is easy to makemistakes. Therefore, the proposed algorithm focuses on considering those errors to overcome.

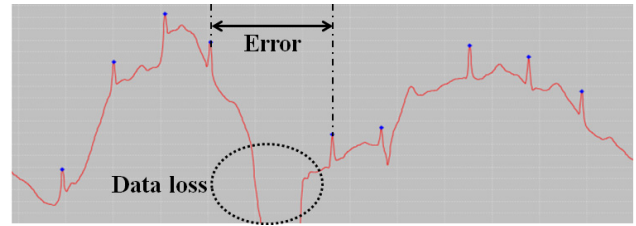


Figure 3. ECG waveforms with data loss

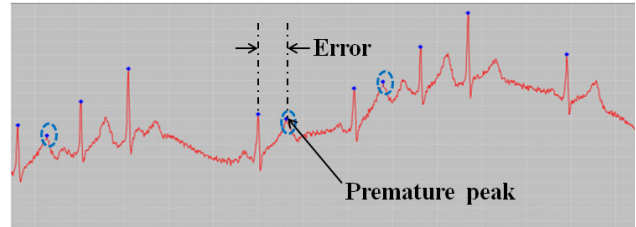


Figure 4. ECG waveforms under motion artifacts or respiration conditions

2.2.2 Algorithm

The proposed algorithm is a modified algorithm that was studied in previous work for real-time peak detection of PPG signals [17]. Figure 5 shows the operation of the proposed R-peak detection method.

In this method, a threshold distance that was described in Equation (6) is used to detect R-peak as following:

The reference distance is an adaptive value, d_{adt} , given by Equation (1).

In Equation (1), K is a dynamic value that depends on the peak-peak amplitude (VP-P) of the AC component in the PPG signal; n is the number of samples from the last local extreme point to the current point; hc is the current heart rate; fs is the sampling frequency. With each new detected R-peak, If EP_{pos} , which is the distance from the previous R-peak point to the current one, is lower than RP , the peak is considered to

be a fake point and is removed as shown in Figure 6. Therefore, the problem in Figure 4 will be solved. In the proposed method, refractory period (RP) that enables us to determine the premature peaks and d_{th} are empirically chosen as 55% of the previous R-R value and 5% of the previous extreme point amplitude, respectively.

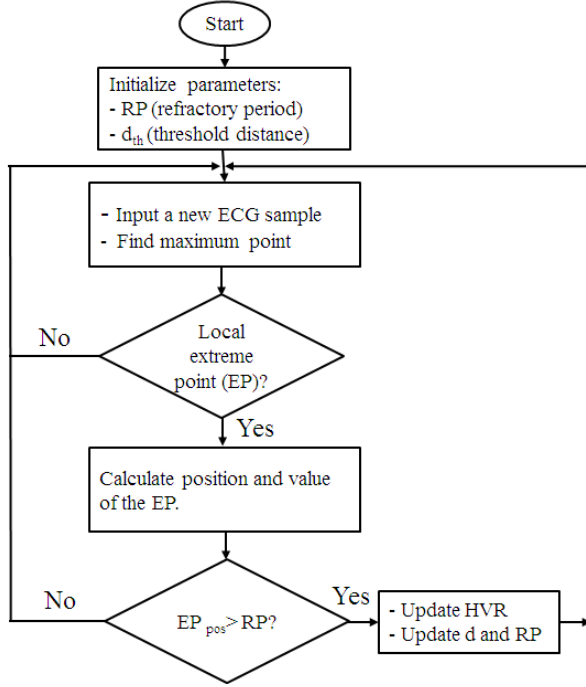


Figure 5. Proposed real-time R-peak detection method

$$d_{adt} = K * \left(1 - \frac{n * h_c}{30 * f_s}\right) \quad (6)$$

The proposed method can accurately detect R-peak of ECG waveforms under challenge conditions and eliminate error peak like premature peaks. However, some error peaks that come from data loss problems as shown in Figure 3 cannot be moved by the proposed method. Therefore, the random error detection method is used to eliminate those error peaks.

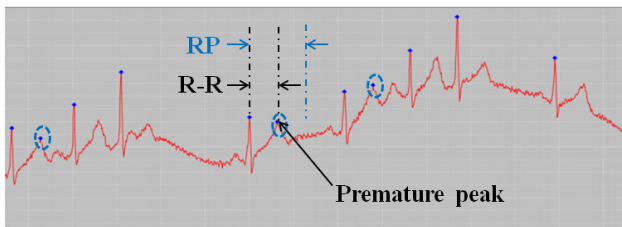


Figure 6. Comparison between R-R and RP for eliminating error peaks

3. System Design & Implementation

The integration of sensing capability into UHF RFID

tags has recently generated a lot of interest among the RFID community^[10,18,19]. In any sensor enabled RFID system data collection is done continuously. Data collection in this context can refer to the computation of statistical means and moments, as well as other cumulative quantities that summarize the data obtained by the system. One of important application areas is healthcare where sensor enabled RFID tags are used in hospitals, clinics, and at home to provide various healthcare services by collecting different environmental and physiological data^[20]. This work also focused on design a health-monitoring system based on RFID technology applying in home healthcare services.

Figure 7 shows the block diagram of the proposed system, including a UHF RFID tag, a MCU, an ECG module, a voltage monitor module, and RF energy harvester. The tag that does not require battery can wirelessly communicate with RFID reader. In this work, the proposed system can be powered by energy from the RF harvester that operates at the frequency of ~915 MHz to collect available RF energy from the reader. However, received RF energy is not always sufficient to supply to the system. Therefore a voltage monitor is designed to manage the power. The proposed ECG sensor tag can collect ECG signal, then the received data are processed and transmitted to the host over the reader as shown in Figure 8.

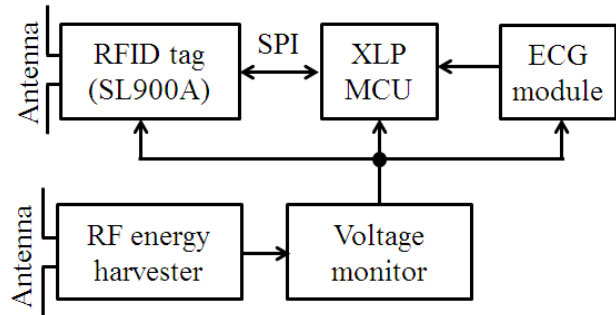


Figure 7. Block diagram of the proposed ECG sensor tag

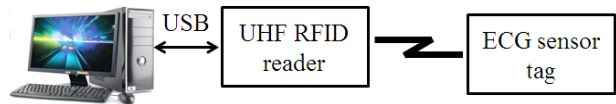


Figure 8. Architecture of the proposed UHF RFID system

3.1 RFID Tag

The RFID tag is built around the SL900A (AMS Co., Australia) that is an EPC global class 1 and class 3 compliant tag chip. Figure 9 shows the block diagram of the tag chip^[21].

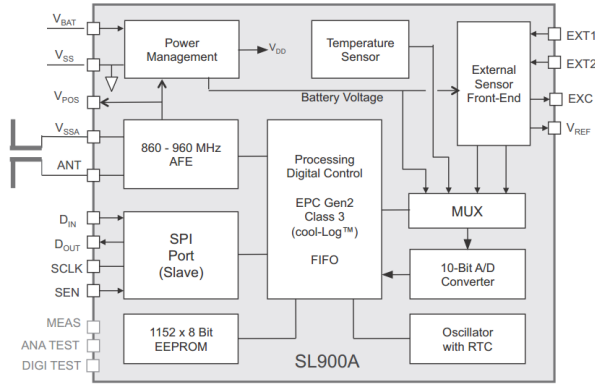


Figure 9. Block diagram of SL900A

The tag chip comprises of some main components: an internal temperature sensor, a SPI interface module for communication data with external MCU (using four signals: Din, Dout, SCLK, and SEN), an external sensor front-end circuit for interfacing with two other external sensors (EXT1 and EXT2), and a power management module that is used to supply voltage from external power in semi-passive mode of the tag. Figure 10 shows the schematic circuit of the proposed tag that can operate in two different strategies, namely, passive mode and semi-passive most. The SPI signals (MISO, MOSI, SCK, SEL) are connected to MCU for receiving ECG data; the battery connector is wired to the RF harvester in semi-passive mode to enhance read range; whereas TP1, TP2 is connected to the tag antenna as shown in Figure 11.

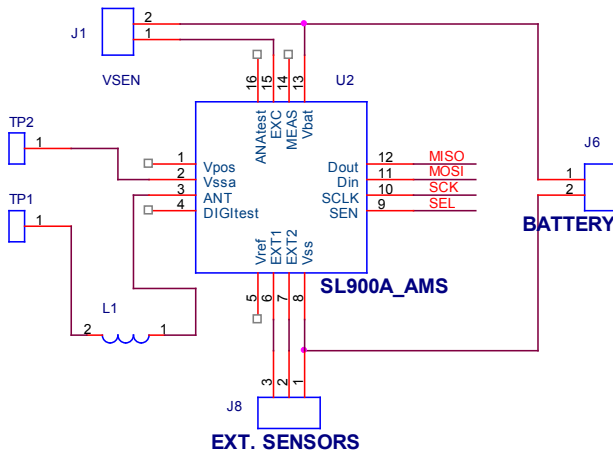


Figure 10. Schematic circuit of the proposed tag

Referring to functions of the SL900A [22], the designed tag antenna has parameters as shown in Figure 11. However, matching inductor (L1) has to be selected to obtain frequency of UHF band for operation of the tag. This study found the best value of 13.4 nH among values from 5.2 nH to 16.4 nH for inductor L1 by using the network analyzer to measure maximum antenna gain at UHF band

(860 MHz ~ 960 MHz) as shown in Figure 12.

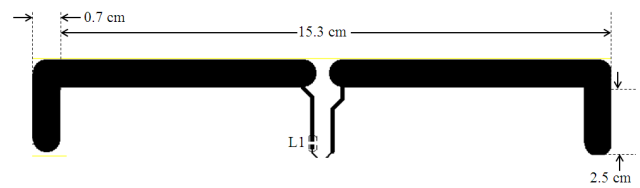


Figure 11. Design of the proposed tag antenna



Figure 12. S11-value of the proposed tag antenna with L1 at 13.4 nH

3.2 MCU, ECG, and Harvester Modules

Figure 13 shows the block diagram for MCU, ECG, and harvester modules. The MCU is created around an extreme low-power microcontroller (PIC16F15xx); the ECG module is based on the ECG circuit that was presented in the next section; whereas the harvester is built around the P1110 (Power Cast Co., USD) that can collect RF energy. In this work, a super-capacitor (C1) whose value is 0.22 F is used to store received power from the harvester. To remain the proposed system in stable operation state, the K-switch is designed to manage the received power. Figure 14 shows the schematic of the K-switch that comprises of a voltage monitor (MAX6264, MAXIM Co.) and a NPN-CMOS transistor. When capacitor voltage is lower a threshold, the K-switch will be off; when the voltage is equal or greater the threshold, the K-switch will be on to supply power to the proposed sensor system.

3.3 The ECG Module

Differences in the speed of wavefront propagation through the cardiac cycle are reflected by different frequencies content of ECG waves. The content of T wave lays mostly within a range from zero (DC) to 10 Hz. The content of P wave is characterized by 5 Hz ~ 30 Hz

frequencies. The content of QRS usually contains within 8 Hz ~ 50 Hz frequencies while abnormal ventricular conduction is characterized by high frequencies (above 70 Hz), forming notches on the QRS. However, the full spectrum of frequencies producing the QRS complex has not been adequately explored. In this study, we chose the frequency of ECG signal from 0.5 Hz to 50 Hz. The proposed ECG circuit is designed using 3 electrodes (LA - left arm, RA - right arm and RLD - GND) as shown in

Figure 15 and Figure 16. The ECG signal obtained from the human body is fed through an IA (Instrument) amplifier, then passed through an HPF (High Pass Filter) filter with a cutoff frequency of 0.2 Hz to filter out baseline noise, then passed to a PA (Power Amplifier) amplifier to increase the signal amplitude, then fed into a 120 Hz LPF (Low Pass Filter) to eliminate high frequency noise before filtering out power line interference using a NF (Notch Filter) to extract the ECG raw signal.

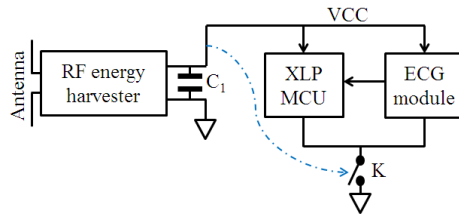


Figure 13. Block diagram of the sensor module with energy harvester

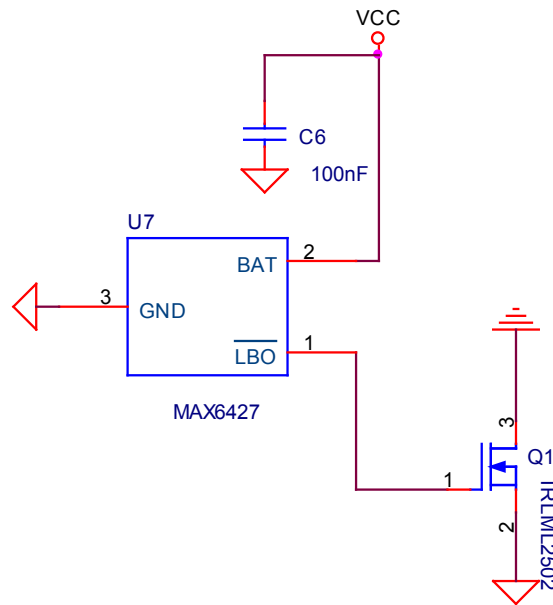


Figure 14. Schematic circuit of the K-switch

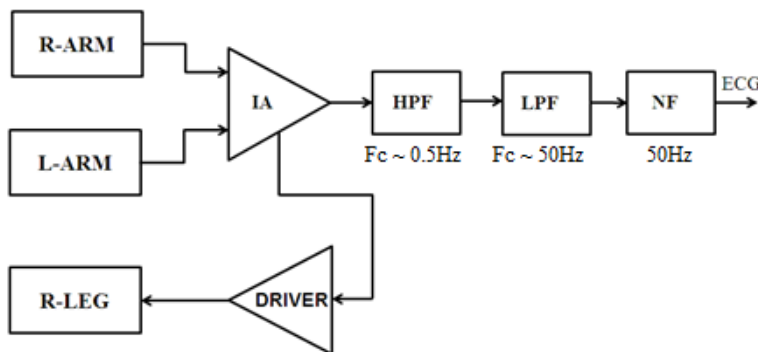


Figure 15. Block diagram of the proposed ECG circuit

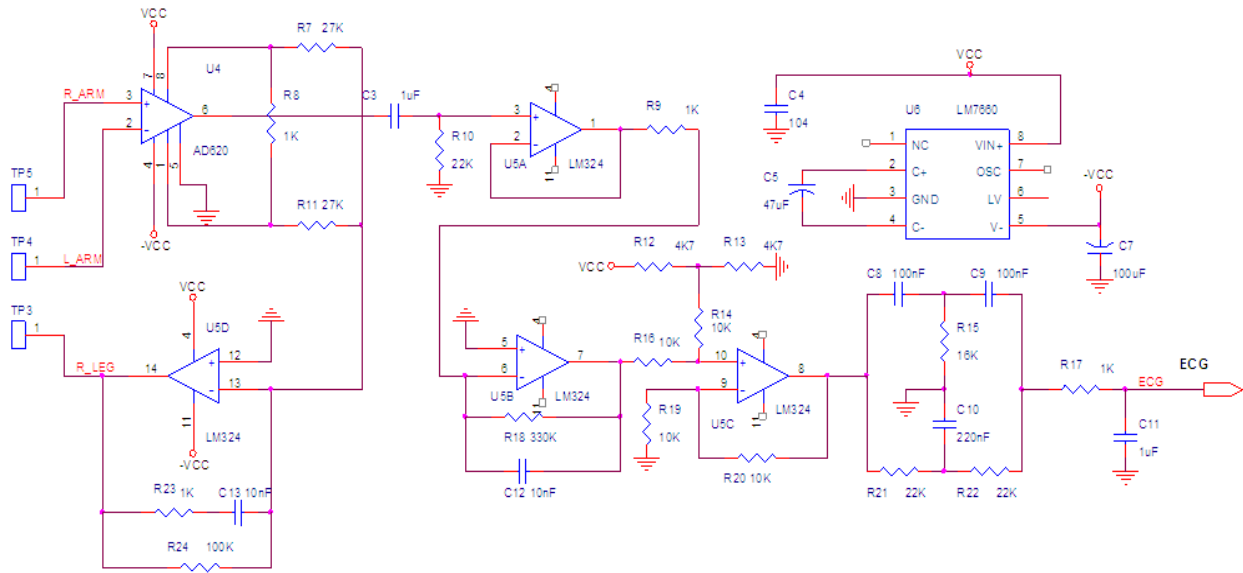


Figure 16. Schematic circuit of the proposed ECG circuit

3.4 The Power Management

The harvesting energy management plays a very important role in voltage distribution to the main power consuming components, the design of which is shown in Figure 17. In this design, the harvested energy is rectified and stored in a 50 mF super capacitor, which is then connected to a 2.1 V voltage lever to close the K1 circuit that powers an MCU. When powered, the MCU controls the power obtained through the voltage divider bridge R1 and R2. When the voltage is enough, the MCU will close K2 to provide the ECG circuit to receive the signal and transmit it to the reader. The harvesting energy control algorithm is shown in Figure 18. When the MCU device is not powered on, the harvester voltage detector checks if $V > 2.1$ V, it will power the MCU, at which point the MCU checks. control energy, when reaching 3.2 V will activate the ECG measuring circuit to work and collect data.

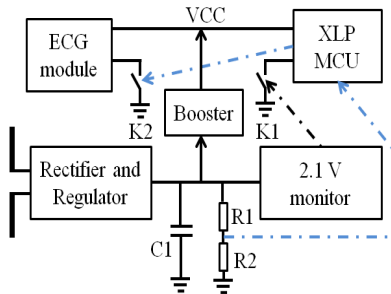


Figure 17. Block diagram of the proposed power manager

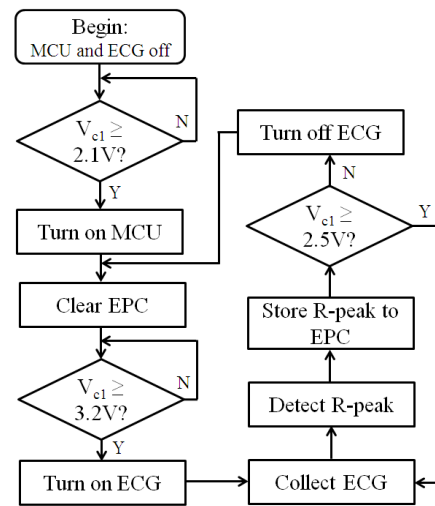


Figure 18. System power controlling

4. Experimental Results

Energy harvesting ECG signal measuring device has been implemented as Figure 19, where Figure 19a is the top side showing upper-capacitor devices (50 mF/5 V) and ECG signal measuring circuit while Figure 19b is the bottom side showing the designed PCB-antenna and the dedicated power harvester, the MCU, the Voltage monitor, and the electrodes. Experimental results are shown from Figure 20 and Figure 21. The results showed that the collected power at distance of 2 m from reader to the proposed ECG sensor. They verified that the proposed system works well with the implemented parameters. The implemented circuit could monitor HRV when it is attached on the human body.

The proposed R-peak detection was coded into the firmware for MCU in the proposed system to detect the peak of the original ECG signals. Figure 22 shows results of the threshold-based method to extract R-peak from ECG raw signal; the results addressed some error peaks due to noise, so that the HRV also have some wrong values (very low val-

ue). Figure 23 shows the results of the proposed algorithm. The results show that premature peaks can be detected. The experimental results highlight the performance of the proposed algorithm under challenge conditions. Therefore the proposed algorithm can be a good solution for real-time R-peak detection in MCU application.

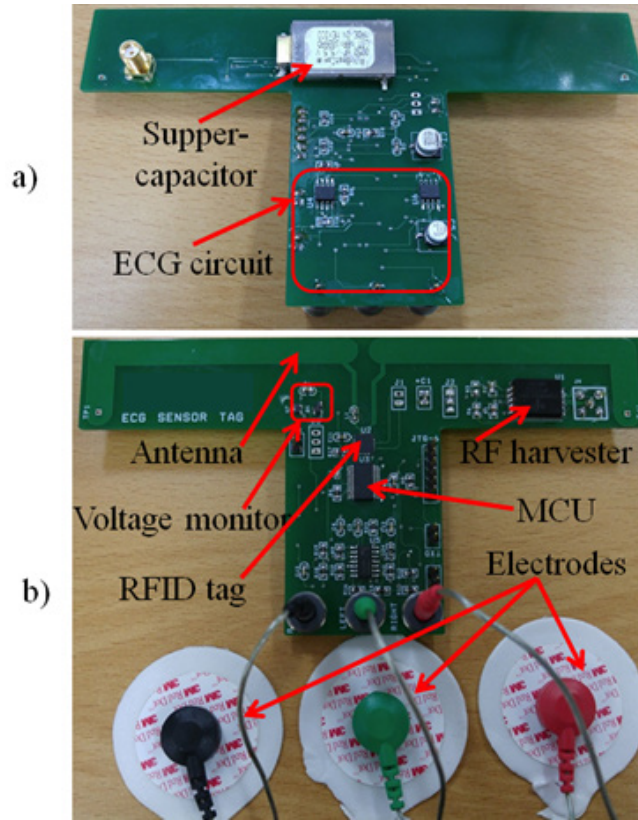


Figure 19. Photograph of the proposed ECG sensor tag; a) top side, b) bottom side

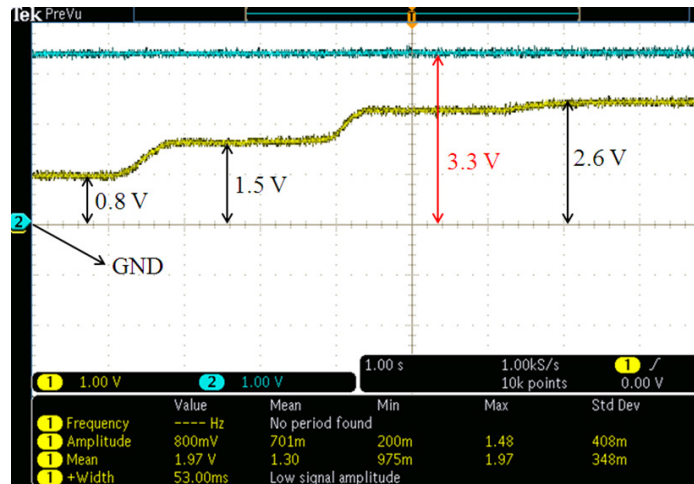


Figure 20. Operation of the boost circuit under various input voltage

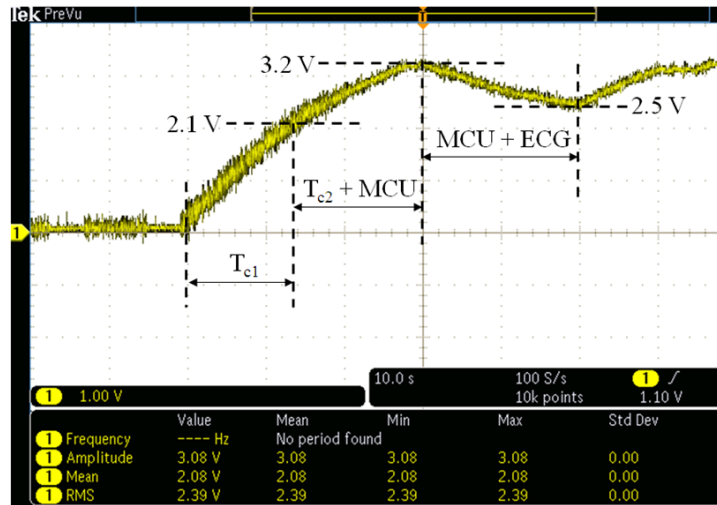


Figure 21. Collected power at distance of 2 m from reader to the proposed ECG sensor tag

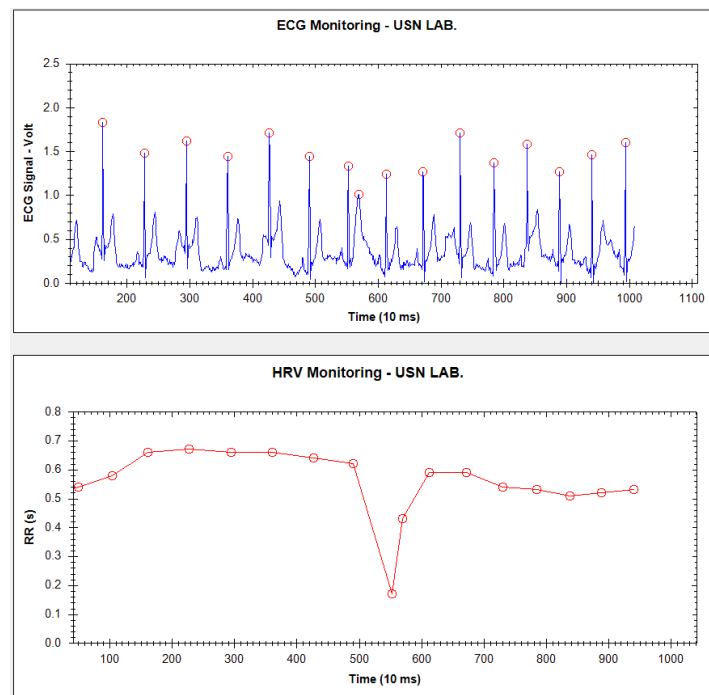


Figure 22. Comparison between R-R and RP for eliminating error peaks

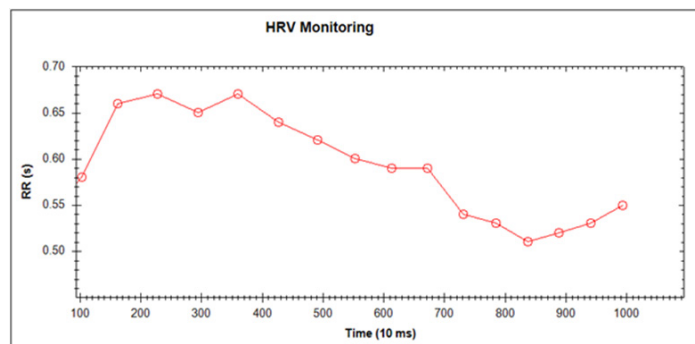


Figure 23. Experimental results of HRV monitoring using the proposed system

5. Conclusions

In this paper, we proposed and implemented a battery less sensing and computational device for monitoring heart rate variability. The implemented system operated well with an ECG circuit that consumes less power of only $\sim 30 \mu\text{A}$ and $\sim 3 \text{ mA}$ on RF harvester at frequency band of 902 MHz \sim 928 MHz. The performance of the proposed system shows that this study can provide a good solution in paving the way to new classes of healthcare applications.

Acknowledgments

This work was supported by FPT University, Hanoi, Vietnam; and Nguyen Tat Thanh University, Ho Chi Minh City, Vietnam.

Conflict of Interest

There is no conflict of interest.

References

- [1] Amini, N., Xu, W., Li, Z., et al., 2011. Experimental Analysis of IEEE 802. 15. 4 for On / Off Body Communications. pp. 2138-2142.
- [2] Choi, J.S., 2010. Performance analysis of ZigBee-based body sensor networks. 2010 IEEE International Conference on Systems, Man and Cybernetics. pp. 2427-2433.
- [3] Dementyev, A., Hodges, S., Taylor, S., et al., 2013. Power consumption analysis of Bluetooth Low Energy, ZigBee and ANT sensor nodes in a cyclic sleep scenario. Wireless Symposium (IWS), 2013 IEEE International. pp. 2-5.
- [4] Andreozzi, E., Sabbadini, R., Centracchio, J., et al., 2022. Multimodal Finger Pulse Wave Sensing: Comparison of Forcecardiography and Photoplethysmography Sensors. *Sensors*, 22, 1-18.
- [5] Jung, S.J., Chung, W.Y., 2011. Flexible and Scalable Patient's Health Monitoring System in 6LoWPAN. *Sensor Letters*, 9(2), 778-785.
- [6] Choi, Y., Zhang, Q., Ko, S., 2013. Noninvasive cuffless blood pressure estimation using pulse transit time and Hilbert–Huang transform. *Computers & Electrical Engineering*, 39(1), 103-111.
- [7] Karmakar, C., Khandoker, A., Penzel, T., et al., 2014. Detection of Respiratory Arousals Using Photoplethysmography (PPG) Signal in Sleep Apnea Patients. *IEEE Biomedical and Health Informatics*, 18(3), 1065-1073.
- [8] Tran, T.V., Chung, W.Y., 2017. A Robust Algorithm for Peak Detection of Photoplethysmograms Waveforms in Mobile Devices. *Journal of Medical Imaging and Health Informatics* 7(7), 1617-1623.
- [9] Alliance, S.B., 1970. Attachment D: RFID Technology Overview. pp. 1-13.
- [10] Salmeron, J.F., Molina-Lopez, F., Rivadeneyra, A., et al., 2014. Design and Development of Sensing RFID Tags on Flexible Foil Compatible With EPC Gen 2. *IEEE Sensors Journal*, 14(12), 4361-4371.
- [11] Dobkin, D., 2007. The RF in RFID: passive UHF RFID in practice. 1.
- [12] RFID standard <http://www.scansource.eu/en/education.htm?eid=12&elang=en>.
- [13] Liao, Y.J., Na, R.T., Rayside, D., 2014. Accurate ECG R-Peak Detection for Telemedicine.
- [14] Rakshita, M., Das, S., 2017. An efficient wavelet-based automated R-peaks detection method using Hilbert transform. *Biocybernetics and Biomedical Engineering*, 37(3), 566-576.
- [15] Chanwimalueang, T., Von Rosenberg, W., Mandic, D.P., 2015. Enabling R-peak Detection in Wearable ECG : Combining Matched Filtering and Hilbert Transform. pp. 134-138.
- [16] Rooijakkers, M., Rabotti, C., Bennebroek, M., et al., 2011. Low-complexity R-peak detection in ECG signals: A preliminary step towards ambulatory fetal monitoring. International Conference of the IEEE Engineering.
- [17] Tran, T., Chung, W.Y., 2015. A Robust Algorithm for Real-Time Peak Detection of Photoplethysmograms using a Personal Computer Mouse. *IEEE Sensors Journal*, 15(c), 1.
- [18] Paper, S., 2009. An Overview of RFID Technology, Application, and Security / Privacy Threats and Solutions.
- [19] Abdulhadi, A., Abhari, R., 2015. Multi-Port UHF RFID Tag Antenna for Enhanced Energy Harvesting of Self-Powered Wireless Sensors. *IEEE Transactions on Industrial Informatics*, 3203(c), 1.
- [20] Rahman, F., Williams, D., Ahamed, S.I., et al., 2014. PriDaC: Privacy Preserving Data Collection in Sensor Enabled RFID Based Healthcare Services. *IEEE International Symposium on High-assurance Systems Engineering*, pp. 236-242.
- [21] A. AMS company, 2014. Data Sheet of the SL900A. pp. 1-90.
- [22] A. AMS company, 2014. RF Characteristics of The SL900A. pp. 1-9.